Experimental Electrical Characterisation of Thermoelectric Generator using Forced Convection Water Cooling

Raihan Abu Bakar, Baljit Singh, Muhammad Fairuz Remeli*
Faculty of Mechanical Engineering
Universiti Teknologi MARA, Shah Alam, Malaysia
**master_raikun8@yahoo.com*

Ong Kok Seng
Faculty of Engineering and Green Technology
Universiti Tunku Abdul Rahman, Kampar, Malaysia

ABSTRACT

Thermoelectric Generator (TEG) provides unique advantages as compared to other heat engines as it is capable to convert heat to electricity directly without having any moving parts. Furthermore, TEG is compact, simple and noiseless and requires very minimal maintenance. This paper presents an experimental and analytical study of a model consisting of a TEG located between a copper water cooling jacket and an aluminium block which acts as a heat spreader. The copper water cooling jacket was used in this study as water has higher thermal capacity than air. Besides, copper is one of highest thermal conductivity materials. TEG characterisation in term of electrical was investigated in this study. Based on the result, it shows a linear proportion relationship between open-circuit voltage and temperature difference across TEG. The result also clearly shows the power output of TEG increases as the temperature gradient across TEG increases. In addition, the impact of water flowrate on TEG power output was also studied. Based on the finding, there was an optimum water flowrate of 80 ml/s. Further increasing the water flowrate is not favourable as it will not increase power output and may lead to higher pumping power for water circulation. At this optimum water flowrate, the maximum power output obtained is equal to 530 mW when TEG hot-side temperature (T_h) is 180 ℃.

Keywords: *Power Generation; Thermoelectric Generator; Water Flowrate, Characterisation.*

ISSN 1823-5514, eISSN2550-164X
Received for review: 2019-01-15
Accepted for publication:2020-01-28
Published:2020-04-01

Nomenclature

I_L	*Total current drawn in the circuit*
P_{max}	*Maximum TEG power ouput*
P_{TEG}	*TEG power output*
$P_{TEG\text{-}exp}$	*TEG power output obtained through experiment*
Q_c	*Heat transfer rate at TEG cold-side*
Q_h	*Heat transfer rate at TEG hot-side*
R_{TEG}	*TEG electrical internal resistance*
R_L	*External load resistance*
T_c	*TEG cold-side temperature*
T_h	*TEG hot-side temperature*
t	*Time*
$V_{ac\text{-}o}$	*Output voltage of AC variable transformer*
V_{oc}	*TEG open circuit voltage*
V_w	*Water flowrate*
α_{TEG}	*TEG Seebeck coefficient*
$\alpha_{TEG\text{-}exp}$	*TEG Seebeck coefficient obtained through experiment*
α_{wire}	*Seebeck coefficient of volt measuring probe wire*
ΔT_{TEG}	*Temperature gradient across TEG*
κ_{TEG}	*TEG thermal conductance*
v_b	*Bottle volume*

Introduction

Electricity plays a vital role in our daily lives. From providing means of basic necessities such as cooking, heating and cooling to luxury and entertainment which include powering home appliances such as televisions and smart phones. Electricity generation mainly comes from thermal power plants and these power plants burn fossil fuels such as coal and gas to produce electricity [1]. These fossil fuels are not only non-renewable, they also contribute towards global warming.

Furthermore, by using Rankine Cycle or Kalina Cycle, these thermal power plants require intermediate-to-high grade heat to convert into mechanical energy and eventually to produce electricity by rotating turbines and generators. Thermal power plants which harness low grade heat may be possible but it is not economical since there are many equipments and complex system required to convert heat to electricity.

Thermoelectric Generator (TEG) provides a best solution to this, as it is able to harness low grade heat to produce electricity directly with the Seebeck Effect. As shown in Figure 1, two dissimilar thermoelectric materials (p-type and n-type semiconductors) are being sandwiched between two ceramics.

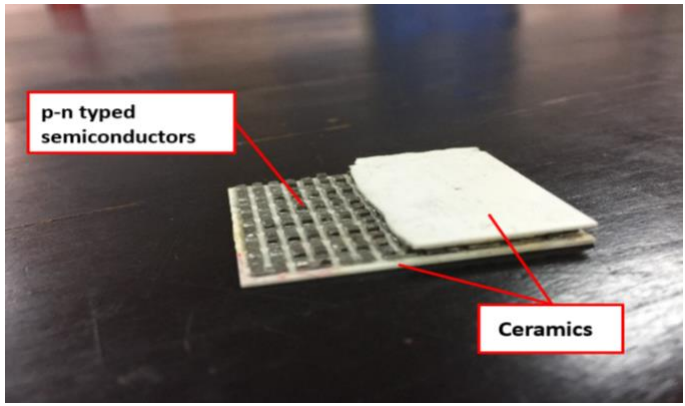

Figure 1: Thermoelectric Generator

While thermal power plants require large space and equipment such as boilers, combustion chambers and turbines to generate electricity, TEG does not require these equipment to generate electricity. In addition, TEG is simple and compact, noiseless, and it requires very minimal maintenance as no moving parts is involved [2].

Nevertheless, the common problems arising with TEG is low power output as well as low electrical efficiency [2]–[7]. TEG material performance is associated with its dimensionless figure of merit:

$$ZT = \frac{\alpha^2}{\kappa\lambda}T \quad (1)$$

where α, κ, λ, T are Seebeck coefficient, thermal conductivity, electrical resistivity and absolute temperature respectively. Low ZT value produces low electrical efficiency and vice versa.

Because of these problems, the use of TEG has been limited to certain applications such as in remote and extreme remote conditions (space exploration), and also in waste-heat recovery [6]. Radioisotope Thermoelectric Generator (RTG) is used in powering two space crafts namely Voyager 1 and 2 started since 1977 until now [8]. RTG produced 158 W at the early stage of the mission. Amerigon, together with its partners (BMW and Fords) carried out a TEG research program for seven years [9]. At the research final stage, they conducted a road test of a cylindrical TEG on two vehicles namely BMW X6 and Lincoln MKT vehicles. Around 450W of power output was obtained as a result of the road test [9].

Nevertheless, numerous studies were carried out to increase TEG efficiency. One of methods is to increase ZT value by performing rare earth

element doping on TEG material. Ivanov et al. [10] investigated Lu and Tm doping effect and TEG performance. The doping result showed a significant increase of *ZT* value. Meanwhile, Zianni [11] demonstrated *ZT* enhancement by proposing width-modulated Si nanowires. The author found out as a constriction width (which modulates the nanowire) decreased, *ZT* value of modulated nanowires increased remarkably.

Most of the time, power output produced by TEG depends on the temperature gradient across it. The higher the temperature gradient, the higher the power output produced by TEG. Kiflemariam and Lin [12] researched the self-cooling mechanism for an array of TEG modules. The power generated by TEGs is able to run a fan which cools down the device temperature up to 20%. Tu et al. [13] explored utilising phase change material (PCM) on TEG for space exploration application purpose. Under a wide range of temperature (from +100℃ to -50℃), the researched showed that 32.32% increase of total power output by using paraffin/5% wt% EG composite. El-Adl et al. [14] investigated passively cooled techniques on TEG performance. These techniques are free convection (FC), passive water cooling (PWC) and vapor phase change cooling (VPC). It was observed that VPC with fins resulted the best performance whereas FC without fins resulted the worst performance. On using different type of cooling fluid besides air and water, a study was conducted by Karana and Sahoo [15] on the impact of two nanofluid coolants on TEG performance for automobile waste heat recovery application. By using MgO nanofluid and ZnO nanofluid, power output improved by 11.38% and 9.86% respectively than using EG-W as coolant. Rezania et al. [16] studied the coolant flowrates on power output of a TEG with micro channel heat sink. There is an optimum flowrate which resulted in maximum net power (the difference between TEG power output and pumping power). Singh et al. [4] performed a similar indoor experiment to determine optimum parameters for TEG performance. They achieved TEG performance of 4.19W power output and 2.62% efficiency at temperature difference of 94.55°Cand 245.25 kPa compressive force.

Based on the previous literatures, to the best of our knowledge, there is a lack of study in determining an optimum water flowrate in TEG electrical characterisation test. Therefore, in this study, the test was carried out by varying water flowrate to determine the optimum water flowrate. Besides, a theoretical model was established to predict the TEG power output. The TEG characterisation test was carried out through a controlled and indoor experiment. In this study, a copper water cooling jacket was used as TEG heat sink. This is due to the fact that water has higher heat capacity than air [17]. Besides, copper is one of highest thermal conductivity materials [18]. In addition, the impact on TEG power output and characteristics was evaluated with broader ranges of water flowrate and temperature difference across TEG as compared to smaller ranges in the study carried out by Singh et al. [4].

Methodology

Design

Figure 2 shows a schematic design of proposed TEG characterisation experiment. In this experiment, a TEG was placed between a copper water cooling jacket and an aluminium block. The aluminium block, inserted with two cartridge heaters, acts to spread heat to the hot side of TEG uniformly. The cartridge heaters are connected in parallel to an AC variable transformer. Temperature input of cartridge heaters was varied by varying output voltage of AC variable transformer. Small protrusions were made on top of aluminium block in order to prevent the TEG from sliding on the block surface, thus effective heating can be achieved. The copper water cooling jacket was placed on top of TEG and the water flowed continuously through it. Thermal paste was applied between TEG and aluminium block to increase heat conduction by reducing thermal contact resistance.

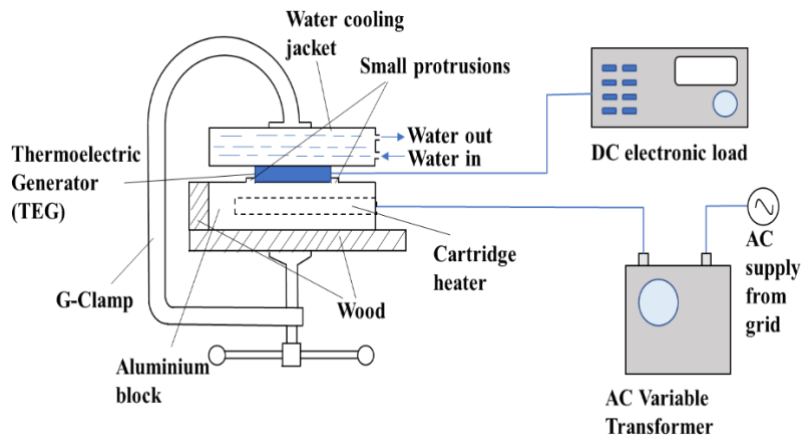

Figure 2: A schematic design of proposed TEG characterisation experiment

Mathematical Model

A mathematical model was developed to analyse the performance of TEG. Several assumptions were made for a simplification purpose:

1) Thermal contact resistances between aluminium block and TEG and between TEG and water-cooling jacket are neglected
2) Heat loss due to convection and radiation is negligible

3) The Seebeck coefficient, thermal conductivity and electrical resistivity of TEG are assumed to be constant; the influence of temperature change is neglected.

The amount of heat transferred to the hot side of TEG is defined [2] as follows:

$$Q_h = \alpha_{TEG} I_L T_h - \frac{{I_L}^2 R_{TEG}}{2} + \kappa_{TEG} \Delta T_{TEG} \quad (2)$$

Whereas, the amount of heat transferred from the cold side of TEG is defined [2] as follows:

$$Q_c = \alpha_{TEG} I_L T_c - \frac{{I_L}^2 R_{TEG}}{2} + \kappa_{TEG} \Delta T_{TEG} \quad (3)$$

By applying energy conservation principle and assuming no heat loss surrounding, an energy balance equation can be written as:

$$Q_h = Q_c + P_{TEG} \quad (4)$$

Equation (4) can be rewritten as follows:

$$P_{TEG} = Q_h - Q_c \quad (5)$$

Substituting Equation (2) and Equation (3) into Equation (5), TEG power output can be expressed as:

$$P_{TEG} = \alpha_{TEG} I_L \Delta T_{TEG} - {I_L}^2 R_{TEG} \quad (6)$$

From Equation (6), P_{TEG} is a function of I_L; the value of I_L determines the value of P_{TEG}. The values ofI_L were obtained from by varying R_L using DC electronic load.

As mentioned in [19, 20], the experimental value of Seebeck coefficient of TEG ($\alpha_{TEG\text{-}exp}$) can be obtained by using Equation (7) below:

$$\alpha_{TEG-exp} = \frac{V_{OC}}{\Delta T_{TEG}} - \alpha_{wire} \quad (7)$$

However, for simplicity reason, α_{wire} is assumed to be negligible and Equation (7) reduced to Equation (8):

$$\alpha_{TEG-exp} = \frac{V_{OC}}{\Delta T_{TEG}} \quad (8)$$

The value of TEG internal resistance (R_{TEG}) is equal to load resistance when power output is maximum. By differentiating an equation of experimental power of TEG ($P_{TEG\text{-}exp}$), which is obtained experimentally and equalizing it to zero, the corresponding voltage and current can be determined. Therefore, R_{TEG}:

$$R_{TEG} = \frac{V}{I} \tag{9}$$

Procedure

In order to validate the mathematical model developed in previous section, an experimental set up was built, as shown in Figure 3.

As shown in Figure 4, TEG used in this experiment is Bismuth Telluride with 127 number of junctions. The Bismuth Telluride Seebeck coefficient of one p-n couple is around 190μV/K [4,21], thus TEG Seebeck coefficient (α_{TEG}) is equal to 0.0241V/K. The TEG dimension is 40 mm (length), 40 mm (width) and 3.2 mm (thickness). The TEG is connected to a DC electronic load. By varying load resistance (R_L) from 0 Ω to 900 Ω through the DC electronic load, the voltage and current outputs produced by TEG were also varied. Meanwhile, the copper water cooling jacket used in this experiment is shown in Figure 5.

Water flowed from the nearest water tap into the water-cooling jacket and flowed out to the sink. Water flowrate was varied according to the opening water tap valve. The calculation of water flowrate is based on how long it takes to fill up one 0.5 litre bottle. Time measurement were recorded and repeated for 5 times in order to obtain accurate average time. Table 1 below shows the details of the water flowrate calculation. Six thermocouples were placed at six different locations to measure the temperature at these locations, as illustrated in Figure 6.

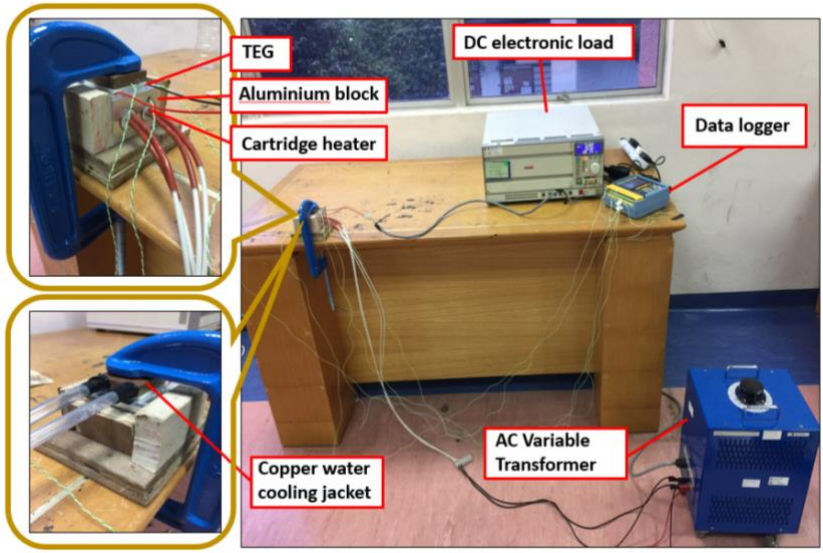

Figure 3: Experimental set up

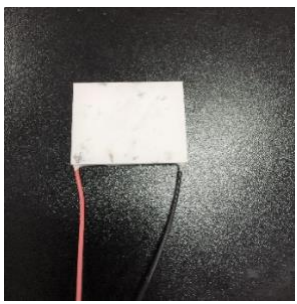

Figure 4: TEG (TEC1-12710T125)

Figure 5: Copper water cooling jacket

Table 1: Water flowrate calculation

Valve Opening	25%	50%	75%	100%
Volume, v_b (litre)	0.5	0.5	0.5	0.5
Average Time, t (s)	32.33	10.27	6.26	4.47
Flowrate,V_w (l/s)	0.015	0.049	0.080	0.112
Flowrate, V_w (ml/s)	15	49	80	112

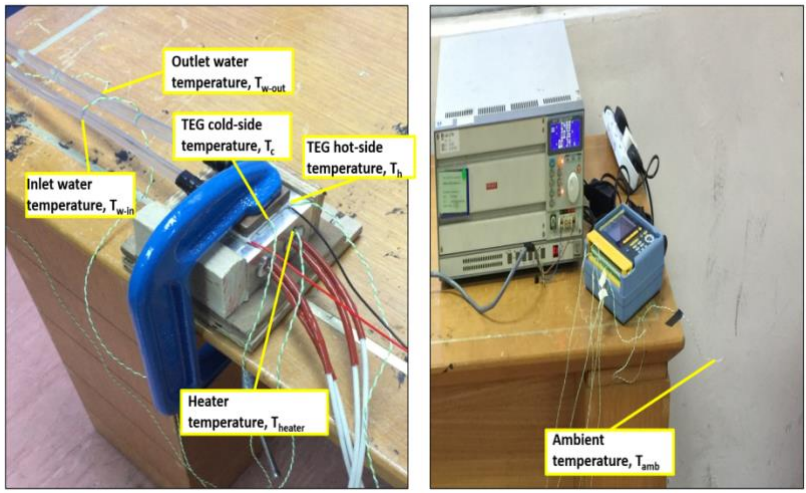

Figure 6: Six different locations of thermocouples

The experiment started by setting output voltage of AC variable transformer ($V_{ac\text{-}o}$) to 60V and with the 25% tap valve opening. Sufficient times were taken to allow all the temperatures to reach steady state condition. Once they reached the steady state condition, all six temperature values were recorded. Also, an open-circuit voltage produced by TEG, V_{oc} (no load condition) was measured.

Then, the load resistance was varied from 0 Ω to 900 Ω by using the DC electronic load and the corresponding voltage and current were recorded. These steps repeated with 50%, 75% and 100% tap valve openings. Finally, the whole experiment was repeated for $V_{ac\text{-}o}$ = 76V, 80V and 100V.

Results and Discussion

Figure 7 illustrates the current and power output curves when the load resistance was varied from 0 Ω to 900 Ω at TEG hot side temperature, ΔT_{TEG} = 53°C and water flowrate, V_w = 15 ml/s. As load resistance increases, the voltage increases whereas the current produced decreases. This inverse linear relationship is clearly shown in Figure 7. The value of experimental power is a product of voltage and current. Power output as a function of voltage is a polynomial curve.

As mentioned in Mathematical Model section, power is maximum when TEG's internal resistance is equal to load resistance. Thus, differentiating an equation $P_{TEG\text{-}exp}$ = -0.0004549V_2 + 0.5504623V + 2.1109526 and equalizing it to zero, V is equal to 605 mV. Corresponding

current value can be determined plugging 605 mV into the equation I = -0.000505V + 0.610009, which is equal to 0.305 A. Thus, by using Equation (9), R_{TEG} value was obtained and is equal to 1.98 Ω.

These R_{TEG} and α_{TEG} values, together with the corresponding current and temperature difference across TEG, were inserted into Equation (6) to obtain theoretical power output. Theoretical power was also plotted in the same graph, as illustrated in Figure 7. It is clearly shown that both theoretical power and experimental power curves are in good agreement. The maximum deviation between these two curves is about 4.05%. This small deviation is probably due to negligence on heat loss to surrounding.

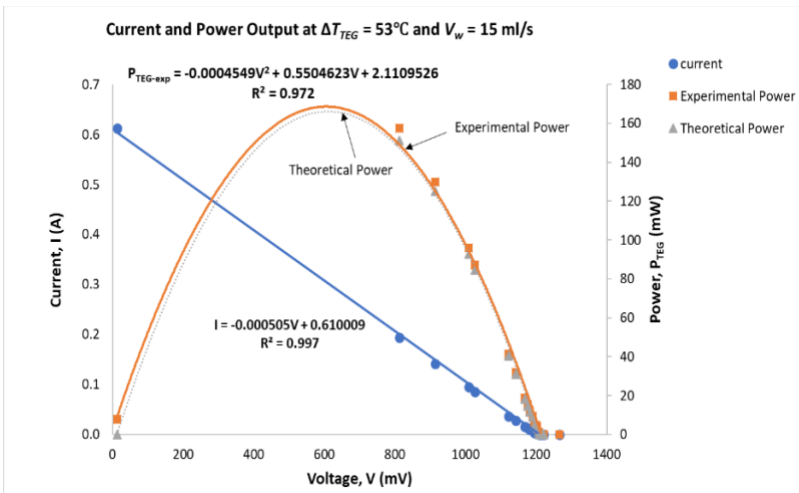

Figure 7: Current and power versus voltage at ΔT_{TEG} = 53 °C and 15 *ml/s*.

Figure 8 shows the effect of water flowrate on power output at different TEG hot-side temperatures. These four graphs in Figure 8 clearly reveal that as water flowrate increases, the power output increases too. However, as water flowrate increases from 80 ml/s to 112 ml/s, an increase in power output is very minimal. Hence, it can be deduced that the optimum water flowrate for this experiment model is 80 ml/s. Further increasing water flowrate will not increase power output. Moreover, it will also cause a negative effect such as higher pumping power for water to circulate. The highest power achieved with this optimum water flowrate at T_h = 180 °C is equal to 530 mW.

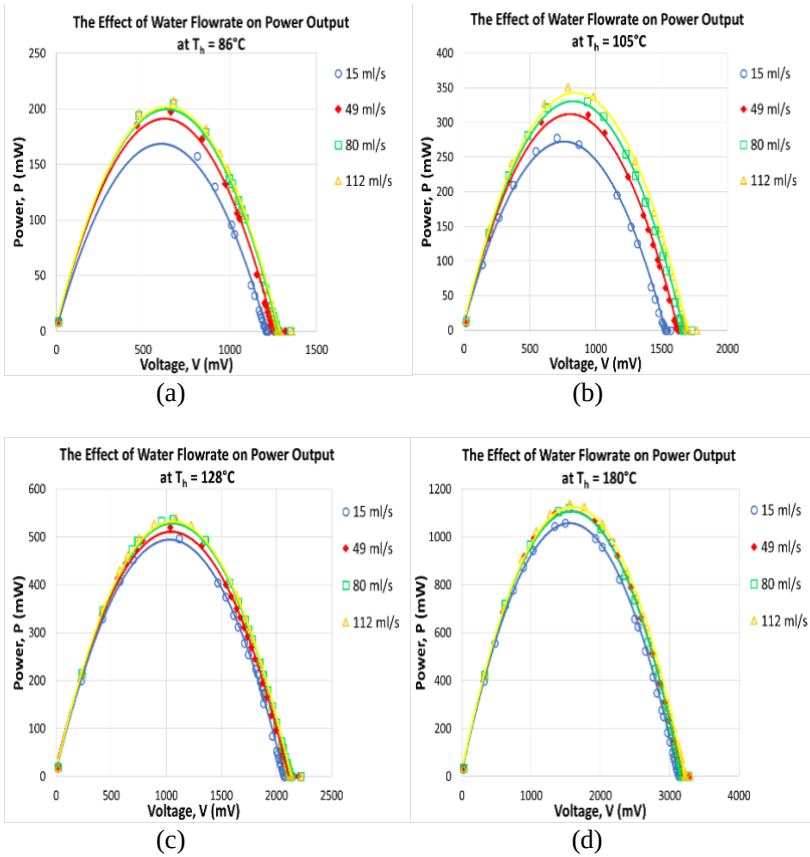

Figure 8: The effect of water flowrate on power output at different TEG hot-side temperatures (a) T_h = 86 °C, (b) T_h = 105 °C, (c) T_h = 128 °C, and (d) T_h = 180 °C.

Figure 9 illustrates current and power curves with four different temperature gradients across TEG at water flowrate, V_w = 15 ml/s, 49 ml/s, 80 ml/s and 112 ml/s. As shown in Figure 9(a), as temperature difference across TEG (ΔT_{TEG}) increases, current and power output produced by TEG also increase. This is also true for other V_w values which are shown in Figure 9(b), 9(c) and 9(d). All I-V curves in Figure 9 have the same slope with very small errors. This means the TEG internal resistance remains constant with different values of hot side temperature and load resistance.

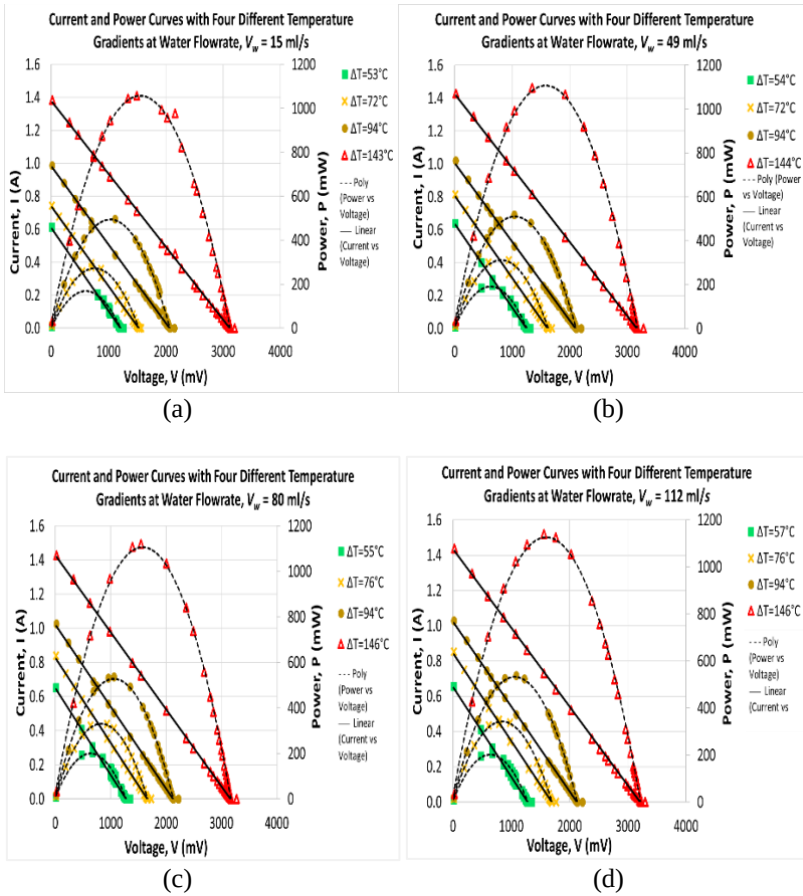

Figure 9: Current and power curves with four different temperature gradients across TEG at different water flowrates (a) V_w = 15 ml/s, (b) V_w = 49 ml/s, (c) V_w = 80 ml/s, and (d) V_w = 112 ml/s.

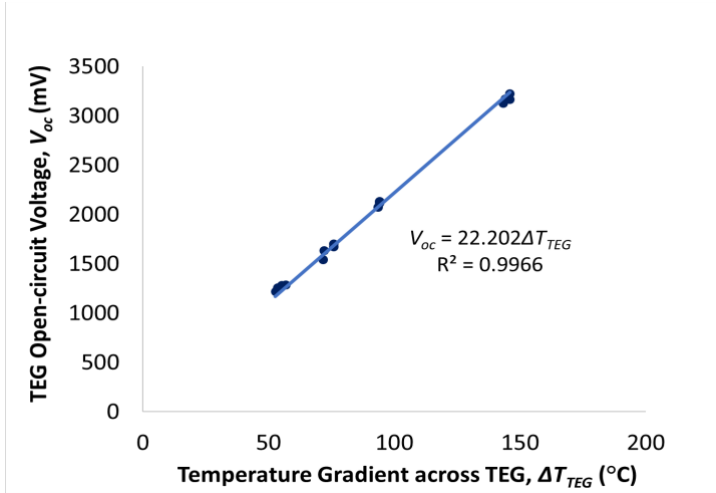

Figure 10: Open-circuit voltage versus temperature difference across TEG.

Figure 10 shows a linear curve of TEG open-circuit voltage (V_{oc}) versus temperature difference across TEG (ΔT_{TEG}). As ΔT_{TEG} increases, V_{oc} also increases linearly.

Figure 11 shows the values of experimental value of TEG Seebeck coefficient $\alpha_{TEG\text{-}exp}$ versus ΔT_{TEG}. These $\alpha_{TEG\text{-}exp}$ values obtained by dividing V_{oc} with ΔT_{TEG}, which are shown in Figure 10. As illustrated in Figure, $\alpha_{TEG\text{-}exp}$ values range from 0.0215 V/K to 0.0236 V/K. This inconsistency is probably due to the fact that Seebeck coefficient varies with temperature [19]–[21]. Also, the estimated Seebeck coefficient value of 0.0241 V/K which was stated previously in Procedure Section is slightly near to this range. Such difference is probably due to previous assumption was made in neglecting the Seebeck effect of volt measuring probe wires. As shown in Equation (7), the estimated Seebeck coefficient value (0.0241 V/K) would have been a bit lower if the Seebeck effect of volt measuring probe wires was taken into consideration.

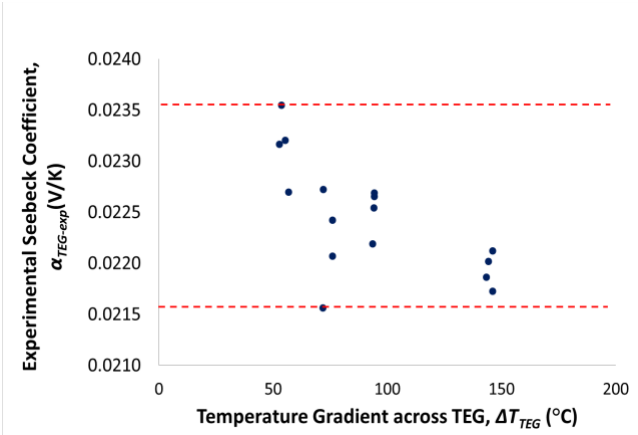

Figure 11: Experimental Seebeck Coefficient versus Temperature Gradient across TEG

Figure 12 illustrates TEG maximum power output, P_{max} versus ΔT_{TEG}. As ΔT_{TEG} increases, P_{max} increases exponentially. A trend line with the following equation was shown in Figure 12 can be used to predict the P_{max} value with a known ΔT_{TEG} value.

$$P_{max} = 0.0001\Delta T_{TEG}{}^{1.8067} \tag{10}$$

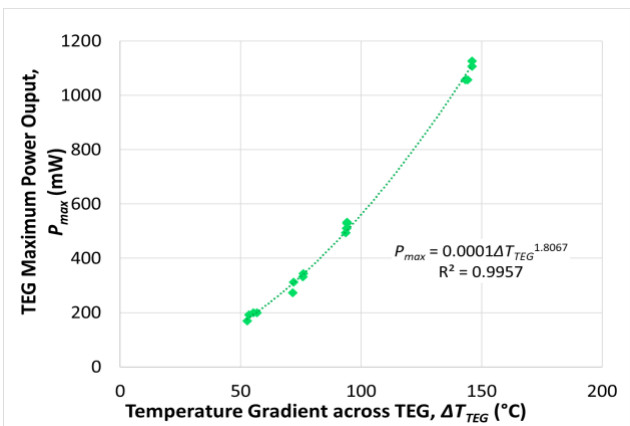

Figure 12: TEG Maximum Power Output, P_{max} versus Temperature Gradient across TEG, ΔT_{TEG}

Conclusion

An experimental setup with one TEG located between a copper water cooling jacket and an aluminium block which acts as a heat spreader was proposed in this study. TEG characterisation in term of electrical characteristics was investigated. The result obtained shows power output by TEG increases as temperature difference across TEG increases. In addition to this, the theoretical power output is also validated with experimental power output, with a maximum difference of 4.05%. Moreover, from this experiment result, we can also conclude that as water flowrate increases, the power output also increases up to a certain flowrate where the power output remains constant. This optimum water flowrate is equal to 80 ml/s. Further increasing water flowrate will not give any advantages on power output. The maximum power achieved with this optimum water flowrate is equal to 530mW when T_h = 180 °C.

References

[1] Agency for Natural Resources and Energy, "Key World Energy Statistics," (2017).
[2] L. J. and K. C. L. Kok S. Ong, "Thermoelectric Energy Conversion," 1, 1–8 (2018).
[3] W. H. Chen, C. Y. Liao, C. I. Hung, and W. L. Huang, "Experimental study on thermoelectric modules for power generation at various operating conditions," Energy 45 (1), 874–881 (2012).
[4] B. Singh, T. Lippong, A. Date, and A. Akbarzadeh, "The effects of temperature difference and compressive force to the electrical characterization of peltier cell for artificial concentrated solar power thermoelectric application," J. Mech. Eng. 11 (1), 15–30 (2014).
[5] D. S. Patil, R. R. Arakerimath, and P. V. Walke, "Thermoelectric materials and heat exchangers for power generation – A review," Renew. Sustain. Energy Rev. 95 (June), 1–22 (2018).
[6] D. Champier, "Thermoelectric generators: A review of applications," Energy Convers. Manag. 140, 167–181 (2017).
[7] G. Liang, J. Zhou, and X. Huang, "Analytical model of parallel thermoelectric generator," Appl. Energy, 88 (12), 5193–5199 (2011).
[8] "Legacy Power Systems | Power and Thermal Systems – NASA Radioisotope Power Systems." [Online]. Available: https://rps.nasa.gov/power-and-thermal-systems/legacy-power-systems/. [Accessed: 17-May-2018].
[9] D. Crane and J. Lagrandeur, "Thermoelectric Generator Performance for Passenger Vehicles," 1–28 (2012).
[10] O. Ivanov, M. Yaprintsev, R. Lyubushkin, and O. Soklakova,

"Enhancement of thermoelectric efficiency in Bi2Te3via rare earth element doping," Scr. Mater. 146, 91–94 (2018).
[11] X. Zianni, "Designing width-modulated Si nanowires for enhanced thermoelectric efficiency," Microelectron. Eng. 159, 51–54 (2016).
[12] R. Kiflemariam and C. X. Lin, "Experimental investigation on heat driven self-cooling application based on thermoelectric system," Int. J. Therm. Sci. 109, 309–322 (2016).
[13] Y. Tu, W. Zhu, T. Lu, and Y. Deng, "A novel thermoelectric harvester based on high-performance phase change material for space application," Appl. Energy 206 (October), 1194–1202 (2017).
[14] A. S. El-Adl, M. G. Mousa, and A. A. Hegazi, "Performance analysis of a passively cooled thermoelectric generator," Energy Convers. Manag. 173 (March), 399–411 (2018).
[15] D. R. Karana and R. R. Sahoo, "Effect on TEG performance for waste heat recovery of automobiles using MgO and ZnO nanofluid coolants," Case Stud. Therm. Eng. 12, 358–364 (2018).
[16] A. Rezania, L. A. Rosendahl, and S. J. Andreasen, "Experimental investigation of thermoelectric power generation versus coolant pumping power in a microchannel heat sink," Int. Commun. Heat Mass Transf. 39 (8), 1054–1058 (2012).
[17] "Heat capacity." [Online]. Available: https://en.wikipedia.org/wiki/Heat_capacity.
[18] H. D. Young, University Physics, 7th ed. (1992).
[19] Z. Zhou and C. Uher, "Apparatus for Seebeck coefficient and electrical resistivity measurements of bulk thermoelectric materials at high temperature," Rev. Sci. Instrum. 76 (2), (2005).
[20] B. Paul, "Simple apparatus for the multipurpose measurements of different thermoelectric parameters," Meas. J. Int. Meas. Confed. 45 (1), 133–139 (2012).
[21] J. Tan et al., "Thermoelectric properties of bismuth telluride thin films deposited by radio frequency magnetron sputtering," 5836, 711–718 (2005).